Contents lists available at YXpublications

International Journal of Applied Mathematics in Control Engineering

Journal homepage: http://www.ijamce.com

An Image Enhancement Method of Power Equipment Based on Fractional Sobel

Caishu Li[a,*], Jian Liu[a]

[a] *Shenyang Jianzhu university, Shenyang, City 110168, China*

ARTICLE INFO

Article history:
Received 20 June 2021
Accepted 30 September 2021
Available online 5 October 2021

Keywords:
Haze image
Sobel operator
Fractional differential
Power equipment
Dark channel prior

ABSTRACT

The study of haze image enhancement of power equipment can effectively find the cause of power system equipment failure and diagnose in time. The traditional haze image enhancement algorithm can not solve the contradiction between image texture details and noise removal. To this end, an algorithm based on the sobel operator fractional model modification combined with dark channel prior is proposed. The texture effect is enhanced by changing the fractional derivative ν value of the fractional differential template of the haze image after denoising processing, which is verified by experiments. The feasibility of the algorithm in this paper is to highlight the texture details while retaining the smooth area in the image, strengthen the target texture information, and relatively improve the accuracy of edge detection.

Published by Y.X.Union. All rights reserved.

1. Introduction

With the gradual improvement of the intelligent level of power system, the method of using remote image and video to evaluate the operation of related equipment in time is becoming more and more common, and the application of computer vision and image processing in power equipment detection is also increasing. However, the climate such as haze and overcast and rain seriously affect the effect of image processing and monitoring. In order to improve the quality of image acquisition in haze environment and reduce the serious impact of dust and fog weather on power equipment imaging system, scholars and researchers at home and abroad have carried out a lot of research on image de-fog processing technology. [1] At present, the classical enhancement algorithms include: histogram equalization, gray transformation, wavelet algorithm, homomorphic filtering algorithm, Retinex algorithm and so on. Usually take the multi-scale information characteristics of the original image as the main consideration, by compensating the contrast, brightness and color saturation of the image scene to eliminate impurities in the non-sensitive areas of the image [2] to achieve the purpose of improving the visual effect of the image. Now the integer order differential operation has been applied to enhance the image, but it loses the texture details of the image while enhancing the image[3], especially the texture of the smooth region loses seriously after the integer order differential, if it is processed by fractional order differential, the texture detail information with little gray change in the smooth region of the image will not be greatly linearly attenuated, and the texture detail information in the smooth region of the image will not be greatly linear attenuated to a certain extent and the order of fractional differential can be changed continuously, so the best image edge information can be obtained by adjusting the order of differential operator in the process of image edge extraction[4].

In this paper, the first-order differential Sobel operator is fractionally improved, and a new fractional edge detection mask is proposed. Combined with the a priori algorithm of dark channel, it retains the advantages of more texture information of the original image and significantly improves the accuracy of defog effect.

2. Principle of image enhancement

2.1 Dark channel a priori

Dark channel a priori is the rule obtained by He through the statistics of a large number of outdoor fog-free images that do not include the sky area, which is based on the observation results in a statistical sense. For an observed image, the dark channel can be expressed as

$$J_{dark}(x,y)=\min_{c\in\{R,G,B\}}\left[\min_{(x,y)\in\Omega(x,y)}\left(J_c(x,y)\right)\right] \tag{1}$$

In the formula, Jc is one of the three color channels R, G, B of an image, c is a color variable, and c is a color variable.

* Corresponding author.
E-mail addresses: 1151434695@qq.com (C. Li)

Ω (x) is the local region of the image; Jdark ((x) is the dark channel; min ( ) of the image is the minimum function.

2.2 Fractional differential

There are many definitions of fractional differential in time domain and frequency domain. There are mainly three classical definitions of fractional calculus, including Gmurl (Grumwald-letnikow), Rmurl (Rieman-Liouville) and Capotu. The fractional differential defined by Gmurl is commonly used in image processing, and its mathematical expression is as follows:

$$ {}_aD_t^v = \lim_{h\geq 0} \frac{1}{h^v} \sum_{m=0}^{\frac{t-a}{h}} \frac{(-1)^m \Gamma(v+1)}{m!\Gamma(v-m+1)} f(t-mh) \quad (2) $$

Where v is the order and zero ∈ (0); h 1) is the step, and an and t are the upper and lower bounds of fractional differentiation, respectively. In the upper and lower bound [a < t], when hackers 1, there is m=t-a. $\Gamma(n)$ is the Gamma function, and the expression is defined as:

$$ \Gamma(n) = \int_0^\infty e^{-t} t^{n-1} dt = (n-1)! \quad (3) $$

2.3 Sobel operator

The traditional Sobel operator is a commonly used gradient amplitude detection operator in edge detection. This operator first uses a 3 × 3 convolution template to weighted average or neighborhood average the detected image, and then uses the first-order differential calculation to detect the edge of the image. The filter operator is as follows:

$$ \boldsymbol{S}_Z = \begin{bmatrix} \boldsymbol{Z}_1 & \boldsymbol{Z}_2 & \boldsymbol{Z}_3 \\ \boldsymbol{Z}_4 & \boldsymbol{Z}_5 & \boldsymbol{Z}_6 \\ \boldsymbol{Z}_7 & \boldsymbol{Z}_8 & \boldsymbol{Z}_9 \end{bmatrix} \quad (4) $$

The corresponding horizontal gradient and vertical gradient operators are as follows:

$$ \boldsymbol{S}_R = \frac{1}{4}\begin{bmatrix} 1 & 0 & -1 \\ 2 & 0 & -2 \\ 1 & 0 & -1 \end{bmatrix}, \boldsymbol{S}_C = \frac{1}{4}\begin{bmatrix} -1 & -2 & -1 \\ 0 & 0 & 0 \\ 1 & 2 & 1 \end{bmatrix} \quad (5) $$

The calculation step of the classical Sobel operator is very simple: in the whole image, two templates are used for convolution, and then the maximum value of the two convolution is assigned to the pixel in the center of the template in the image as the new gray value of the pixel, and then the appropriate threshold is selected, and the pixel whose gray value is greater than TH is the edge point. The advantage of Sobel operator is that the calculation is simple, but the image denoising is not carried out before the convolution operation, and the two first-order differential gradient templates used are not ideal for edge detection. The method to determine the edge point is not very accurate, and it is easy to misjudge.

3. The method of this paper

In this paper, the Sobel operator will be improved and combined with the dark channel a priori method, the improved contents are as follows:

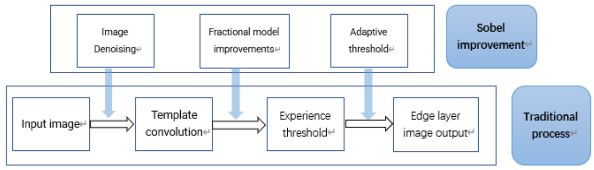

Fig. 1 operator improvement

3.1 Denoising

After inputting the image, we have to convolution the image, and before that, we have to deal with the noise of the image. At this time, we choose the image denoising method based on U-Net fusion in reference [6]. The main purpose is to retain the image texture information and has a good denoising performance, which is proved to be reasonable.

Let the two-dimensional image function be:

$$ G_{(x,y)} = \frac{1}{2\pi\sigma^2} \exp\left(-\frac{x^2+y^2}{2\sigma^2}\right) \quad (6) $$

The gradient vector is

$$ \nabla G = \begin{pmatrix} \partial G / \partial x \\ \partial G / \partial y \end{pmatrix} \quad (7) $$

The decomposition method is used to improve the speed, and two filter convolution templates are decomposed into two one-dimensional row and column filters.

$$ \frac{\partial G}{\partial x} = kx\exp\left(-\frac{x^2}{2\sigma^2}\right)\exp\left(-\frac{y^2}{2\sigma^2}\right) = h_1(x)h_2(y) \quad (8) $$

$$ \frac{\partial G}{\partial y} = ky\exp\left(-\frac{y^2}{2\sigma^2}\right)\exp\left(-\frac{x^2}{2\sigma^2}\right) = h_1(y)h_2(x) \quad (9) $$

Among them, k is constant and σ is the filter parameter, which controls the degree of smoothing the image.

3.2 Based on fractional Sobel operator

Let F (xrem y) be the grayscale value of the denoised point (xrem y) of the image, and take its 3 × 3 pixel range, as follows:

$$ \begin{bmatrix} \boldsymbol{F}(\boldsymbol{x}-\boldsymbol{1},\boldsymbol{y}-\boldsymbol{1}) & \boldsymbol{F}(\boldsymbol{x}-\boldsymbol{1},\boldsymbol{y}) & \boldsymbol{F}(\boldsymbol{x}-\boldsymbol{1},\boldsymbol{y}+\boldsymbol{1}) \\ \boldsymbol{F}(\boldsymbol{x},\boldsymbol{y}-\boldsymbol{1}) & \boldsymbol{F}(\boldsymbol{x},\boldsymbol{y}) & \boldsymbol{F}(\boldsymbol{x},\boldsymbol{y}+\boldsymbol{1}) \\ \boldsymbol{F}(\boldsymbol{x}+\boldsymbol{1},\boldsymbol{y}-\boldsymbol{1}) & \boldsymbol{F}(\boldsymbol{x}+\boldsymbol{1},\boldsymbol{y}) & \boldsymbol{F}(\boldsymbol{x}+\boldsymbol{1},\boldsymbol{y}+\boldsymbol{1}) \end{bmatrix} $$

Then the Sobel operator is improved. Taking the row gradient template as an example, the difference expression is obtained as follows:

$$ G_R(x,y) = \frac{1}{4}\big[F(x-1,y-1) - F(x-1,y+1) + 2F(x,y-1) - 2F(x,y+1) + F(x+1,y-1) - F(x+1,y+1)\big] \quad (10) $$

The image is sampled at equal intervals, and the step size is xcad2, and the approximate differential form of GR (xmemy) is obtained.

$$G_R(x,y) = -\frac{1}{2}\left[\begin{array}{l}\frac{\partial F(x-1,y+1)}{\partial y}+\\ 2\frac{\partial F(x,y+1)}{\partial y}+\frac{\partial F(x+1,y+1)}{\partial y}\end{array}\right] \quad (11)$$

Through further calculation, the approximate expression of binary signal in y direction is obtained.

$$\begin{aligned}\frac{\partial^v F(x,y)}{\partial y^v} &= F(x,y)+(-v)F(x,y-1)\\ &+\frac{(-v)(-v+1)}{2}F(x,y-2)\\ &+\frac{\Gamma(-v+1)}{n!\Gamma(-v+n+1)}F(x,y-n)\end{aligned} \quad (12)$$

$$G_R^v(x,y) = -\frac{1}{2}\left[\begin{array}{l}\frac{\partial^v F(x-1,y+1)}{\partial y^v}\\ +2\frac{\partial^v F(x,y+1)}{\partial y^v}+\frac{\partial^v F(x+1,y+1)}{\partial y^v}\end{array}\right] \quad (13)$$

where $G_R^v(x,y)$ is the improved row gradient. Because the classical Sobel operator template is separated by two rows or two columns, the gray level on both sides of the edge is enhanced, but the resulting edge appears to be too thick. In order to achieve better edge detection processing without causing a large error, it is improved to select the first three terms of the differential definition formula (12) of the fractional differential with a step size of x × 1 in order to form a 3 × 3 mask. The difference approximate expression of equation (13) is obtained as shown in formula (14).

Inspired by the fractional differential theory, we extend the integer order (first order) differential operation in parallel to the fractional order, and the new model is as follows:

$$\begin{aligned}G_R^v(x,y) = -\frac{1}{2}\Big\{&F(x-1,y+1)+2F(x,y+1)+\\ &F(x+1,y+1)+(-v)\\ &\left[F(x-1,y)+2F(x,y)+F(x+1,y)\right]\\ &+\frac{(v^2-v)}{2}\left[\begin{array}{l}F(x-1,y-1)\\ +2F(x,y-1)+F(x+1,y-1)\end{array}\right]\Big\}\end{aligned} \quad (14)$$

So the gradient of the fractional model of Sobel operator is:

$$G^v(x,y) = \sqrt{\left(G_R^v(x,y)\right)^2+\left(G_C^v(x,y)\right)^2} \quad (15)$$

Where $G_C^v(x,y)$ is a similar fractional column gradient, the improved horizontal and vertical gradient templates are as follows:

$$\begin{aligned}S_R^v &= \frac{1}{2}\begin{bmatrix}\frac{v-v^2}{2} & v & -1\\ v-v^2 & 2v & -2\\ \frac{v-v^2}{2} & v & -1\end{bmatrix},\\ S_C^v &= \frac{1}{2}\begin{bmatrix}-1 & -2 & -1\\ v & 2v & v\\ \frac{v-v^2}{2} & v-v^2 & \frac{v-v^2}{2}\end{bmatrix},\end{aligned} \quad (16)$$

Here, the selection of the parameter v plays an important role in extracting the edge of the image texture.

3.3 Adaptive threshold

The selection of threshold is very important in edge detection, which directly determines the result of edge detection. If the threshold is too high, the edge may not be found or the edge may not be completed; if the threshold is too low, the edge will become thicker and contain a lot of noise, and the appropriate threshold will achieve the desired effect. The selection of classical Sobel operator threshold TH is mostly based on multi-person experience, so it is difficult to obtain high-precision edge data. The adaptive threshold selection method is proposed in reference [6]. Similarly, we give an adaptive threshold selection principle as the threshold of the improved Sobel operator.

$$\mathrm{T} = 4\sum_{i=1}^{M}\sum_{j=1}^{N}G^v(x,y)/(MN) \quad (17)$$

M and N are the number of rows and columns of the image, respectively. As can be seen from the above formula, T is actually 4 times the average gradient of the whole image. In other words, if the gradient of a pixel is more than four times larger than that of a normal image, the pixel is an edge point.

3.4 Defog algorithm

(1) Calculate dark channels and transmission graphs:

In order to get a clear image after defog, it is necessary to calculate the transmittance t and atmospheric light intensity A under the condition that the fog graph G (xpeny) is known, so as to restore a clear image J (xpeny).

The algorithm in this paper draws lessons from the dark channel a priori image defog method proposed by He. For the local region of the RGB image which does not include the sky region, there are at least one color channel with some pixels whose brightness is very low and close to zero. That is, for any natural fog-free image, the dark channel of J (x) can be expressed as

$$J_{dark}(x) = \min_{y\in N(x)}\left[\min_{c\in\{R,G,B\}}\left(J_c(y)\right)\right] \quad (18)$$

Therefore, for an image G (xrecoery y), its dark channel based on fractional differential can be expressed as:

$$G_{dark}(x,y) = \min_{c\in\{R,G,B\}}\left[\min_{(x,y)\in\Omega(x,y)}\left(f_{conc}G_c(x,y),g\right)\right] \quad (19)$$

Where: $f_{conc}(\ )$ is the convolution calculation, that is, one of the color channels of the image is convolved with the fractional differential enhancement operator; N(x) is the local area; $\Omega(x,y)$ is the (x,y) range; g is the differential obtained by the improved Sobel operator.

According to the literature (combination), we can know the atmospheric light value A: select the lower proportion of the highest brightness pixels, and then correspond the above points to the same position pixels of the original image J (x), and select the maximum RGB component averaging of each pixel in the original image as the atmospheric light value. From the atmospheric scattering model, the following results can be obtained:

$$\frac{G(x,y)}{A} = \left(1 - t(x,y)\right) + \frac{J(x,y)t(x,y)}{A} \tag{20}$$

Minimize the above formula

$$\begin{aligned}\min_{(x,y)\in\Omega(x,y)}\left[\min_{c\in\{R,G,B\}}\frac{G_c(x,y)}{A_c}\right] &= \left(1 - t(x,y)\right)\\ &+ \min_{(x,y)\in\Omega(x,y)}\left[\min_{c\in\{R,G,B\}}\frac{J_c(x,y)}{A_c}\right]t(x,y).\end{aligned} \tag{21}$$

In the formula, $G_c(x,y)$ is the image containing haze, and the meaning of the image color value $c\in\{R,G,B\}$, Gdark can be inferred; A_c is the global atmospheric light intensity; $J_c(x,y)$ is the clear image after defog.

According to the a priori theory of dark channel, it is known that the brightness of the dark channel pixel of the fog-free image is very small, which is close to 0, and the luminance value of the dark channel pixel in the fog image is very close to the fog concentration value, so the atmospheric light intensity can be estimated by using the dark channel value of the image, and then the atmospheric transmittance $t(x,y)$, can be obtained.

$$t(x,y) = 1 - \min_{(x,y)\in\Omega(x,y)}\left[\min_{c\in\{R,G,B\}}\frac{G_c(x,y)}{A_c}\right] \tag{22}$$

If the atmospheric light intensity value A_c is a known value, the estimated atmospheric refractive index in the neighborhood of $\Omega(x,y)$ can be obtained by taking $J_c(x,y)=0$,.

$$\tilde{t}(x,y) = 1 - \min_{(x,y)\in\Omega(x,y)}\left[\min_{c\in\{R,G,B\}}\frac{G_c(x,y)}{A_c}\right] \tag{23}$$

The calculation method of A_c in this paper is to extract the first 0.1% pixels according to the luminance from the dark channel map of R, G and B, and then take the value of the pixel with the highest intensity in the extracted 0.1% pixel as the atmospheric light value of each channel, and then take the average atmospheric intensity value of R, G and B as the atmospheric light intensity value of this paper.

$$A_c = \frac{1}{3}\sum_{c\in\{R,G,B\}}\max\left[\max\left(G_{dark,c}(x,y),0.1\right)\right] \tag{24}$$

where $\max(\ )$ is a maximum function.

(2) Haze image enhancement:

Using the previous calculation, the transmission picture $t(x,y)$ and the global atmospheric light intensity are obtained, and the enhanced image can be obtained.

$$\begin{aligned}J(x,y) &= \frac{G(x,y) - \max\left[\max\left(G_{dark,c}(x,y),0.1\right)\right]}{\tilde{t}(x,y)}\\ &+ \frac{1}{3}\sum_{c\in\{R,G,B\}}\max\left[\max\left(G_{dark,c}(x,y),0.1\right)\right]\end{aligned} \tag{25}$$

In order to prevent the situation where $\tilde{t}(x,y)$ is zero, the lower limit value t_0 (t_0 is generally set to 0.1), that is, $\max\left(\tilde{t}(x,y)t_0\right)$ is used instead of $\tilde{t}(x,y)$;, so the final expression of $J(x,y)$ can be obtained:

$$\begin{aligned}J(x,y) &= \frac{G(x,y) - \max\left[\max\left(G_{dark,c}(x,y),0.1\right)\right]}{\max\left(\tilde{t}(x,y),t_0\right)}\\ &+ \frac{1}{3}\sum_{c\in\{R,G,B\}}\max\left[\max\left(G_{dark,c}(x,y),0.1\right)\right]\end{aligned} \tag{26}$$

4. Analysis of experimental results

4.1 Selection of experimental parameters

In order to verify the effect of the introduced fractional differential operator on image defog, two images are randomly selected and the algorithm proposed in this paper is used to defog. The changes of the transmittance and the image effect after defog enhancement are given when v in the fractional differential enhancement operator takes different values between 0: 1, respectively.

(a) Image 1 original (b) v = 0.1 Image 1

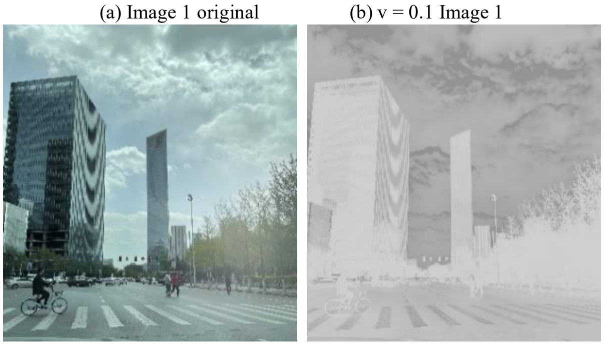

(c) v = 0.1 enhanced image 1 (d) v = 0.5 image 1

(e) v = 0. 5 enhanced image 1 (f) v = 0. 9 image 1

(f) v = 0.9 enhanced image 1

Fig. 2 The original image with different v values in image 1 and the enhanced image

(a) Image 2 original (b) v = 0.1 Image 2

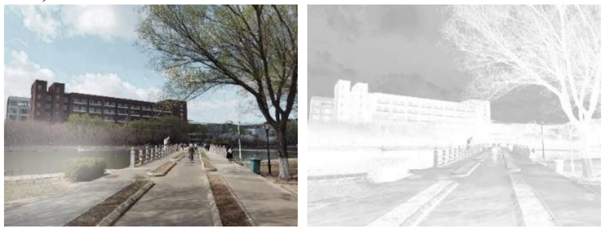

(c) v = 0.1 enhanced image 2 (d) v = 0.5 image 2

(e) v = 0. 5 enhanced image 2 (f) v = 0. 9 image 2

(f) v = 0.9 enhanced image 2

Fig. 3 The original image with different v values and the enhanced image in image 2

Peak signal-to-noise ratio ((peak signal to noise ratio, PSNR), average gradient, information entropy and structural similarity, which are commonly used to evaluate image quality, are used as quantitative evaluation criteria for image enhancement results. Among them, PSNR is used to evaluate the noise reduction of the processed image, and the larger the PSNR value is, the smaller the distortion of the image is, the better the integrity of its structure is, and the higher the noise suppression degree of the algorithm is; the average gradient reflects the ability of the image to express the contrast of small details, and is used to evaluate the blur degree of the image, the larger the average gradient is, the more texture information of the image is, and the clearer the image is. Information entropy is used to represent the amount of information provided by an image. The greater the value of information entropy, the more information the image contains, and the better the image quality is under the condition of the same texture level and sharpness index. Structural similarity is an index to measure the similarity of two images. From the point of view of image composition, structural information is defined as attributes that reflect the structure of objects in the scene independent of brightness and contrast. The greater the value of structural similarity, the stronger the ability to retain the structural information integrity of the original image, and the more obvious the improvement effect on fog. The experimental results are shown in the table below.

Table 1 Evaluation indicators corresponding to different threshold images

Test image	v	PSNR	Averae gradiet	Information entropy	Structural similarity
1	0.1	14.16	5.18	12.73	0.62
	0.3	11.33	4.84	12.18	0.54
	0.5	9.40	4.51	10.79	0.46
	0.7	8.26	3.39	9.85	0.36
	0.9	7.42	3.43	8.20	0.43
2	0.1	16.43	4.12	10.08	0.72
	0.3	14.32	4.96	11.36	0.69
	0.5	11.80	5.86	12.65	0.66
	0.7	10.03	6.11	13.56	0.52
	0.9	8.71	5.87	13.11	0.71

From the table above, it can be seen that the change of the transmittance map of the foggy image is very obvious when v is taken with different values, and the defogged image corresponding to different transmittance is also different. This is mainly because different image acquisition processes are affected by the environment (such as light, fog and other factors), so the image transmittance is also different. The transmittance obtained by the traditional image de-fog enhancement algorithm based on atmospheric scattering theory is based on statistical method, so the unique transmittance of an image can only be obtained, but it must be the best. For the foggy images of different scenes, it is very necessary to take the relatively clear images with different values after enhancement.

4.2 Defog experiment of power equipment

The haze image enhancement results obtained in this paper are compared with the classical histogram equalization algorithm, Fattal algorithm and He algorithm. The following picture shows the enhancement effect of foggy image processed by various foggy image algorithms. According to the simulation results of the graph, the foggy images of different scenes are obviously different after being processed by different algorithms.

Compared with the experimental results of the image, we can see that the local area of the image processed by He algorithm is dark, and there are a lot of noise areas, and some insulators in figure 3 become difficult to identify; after the image is enhanced by Fattal algorithm, the image contains more dark areas, and the part of the box processed by Fattal algorithm can hardly recognize the specific content of the included object. In contrast, the algorithm in this paper can well show the power meter contained in the image, which can prove that the image processed by this algorithm can show more detailed information.

Figure 4 contains the image of the power line and the support frame, it can be found that the power line in the original image is almost invisible, but it becomes much clearer after the algorithm and histogram equalization algorithm. Through further observation, it can be found that the color of the image after removing fog by using this algorithm is relatively light, and the image when it is close to natural fog-free appears more natural; the sky part of the image after removing fog by histogram algorithm appears sunset-like color, which is over enhanced for the sky part.

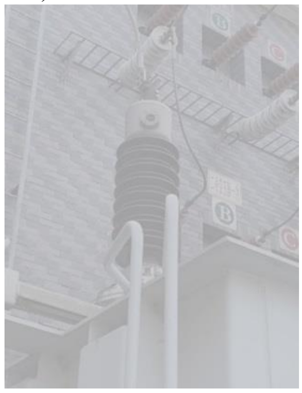


(b) He algorithm for (a) original Image

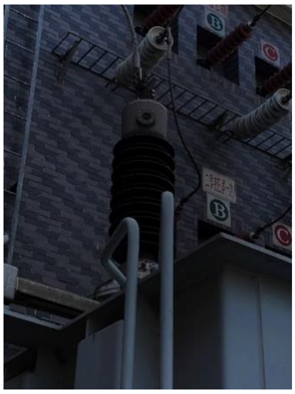


(c) Fattal algorithm (d) algorithm in this paper

Fig. 4 Image processing results of different algorithms


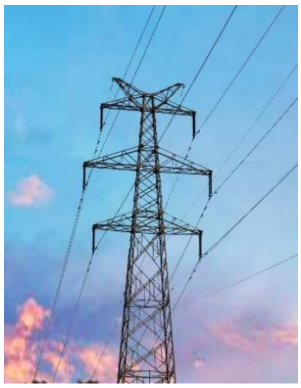

(b) histogram algorithm for (a) original Image

(c) algorithm in this paper

Fig. 5 Image processing results of different algorithms

Through the reference [7], we can use the method of objective evaluation to compare the performance of each algorithm, and calculate the relative comparison, edge similarity and joint value of each algorithm between the restored image and the original atomized image. The results are shown in the following table:

Table 2 the first set of image quality evaluation indicators

	Original image	He	Fattal	Algorithm in this paper
Relative contrast of defog image	0.1053	0.3927	0.4136	0.4754
Edge similarity of defog image	0.5127	0.8431	0.8153	0.8872
Defog image joint value	0.1011	0.3523	0.3294	0.4862

Table 3 the second group of image quality evaluation indicators

	Original image	Histogram equalization algorithm	Algorithm in this paper
Relative contrast of defog image	0.2342	0.3489	0.3892
Edge similarity of defog image	0.7194	07018	07583
Defog image joint value	0．1937	00.1975	0.2927

It can be seen from the table that the joint values of relative contrast and edge similarity of the restored images obtained by this algorithm are higher than those of other defog algorithms. It is further proved that this algorithm has certain advantages for haze image processing of electric power engineering site construction.

It is not difficult to imagine that for the visual management and control system of electric power construction and the fault identification of UAV power patrol, the video images collected in low light and foggy environment are processed by this algorithm, and then input into the image detection and recognition system for detection and recognition. undoubtedly, it can greatly improve the efficiency of power engineering management and control and the accuracy of fault identification. Reduce the input of manpower and material resources in the process of visual engineering management and control and power fault identification and detection.

5. Conclusion

In this paper, according to the definition of fractional differential, the integer order Sobel operator is transformed into a fractional order operator, and the Sobel operator is improved, which ensures the texture of the image in image processing. Combined with the dark channel prior algorithm, experiments are carried out on the haze image of power equipment. The experimental results show that the algorithm effectively improves the image quality and strengthens the target information. This algorithm not only has a good effect on foggy image enhancement. It has a high degree of noise suppression, and can retain the structure and color information of the original image, and there will be no color distortion, halo effect and other problems.

Acknowledgements

Thanks to the national key R&D project 2020YFC0833203 and the Jiangsu Provincial Construction Laboratory Open Project JSKLESS201707 for supporting this project.

References

[1] Wang Hao, Zhang Ye, Shen Honghai, et al. Overview of image enhancement algorithms [J]. China Optics, 2017 10 (4): 438-448.

[2] Huling, Chang Xia, Ji Feng. New progress in image edge detection [J]. Modern Electronic Technology, 2018. 41 (23): 32-mm.

[3] Guo Rui, Party Jianwu, Shen Yu, et al. Image sharpening algorithm for foggy sky based on multi-scale geometric analysis [J]. Advances in Laser and Optoelectronics, 201855 (11): 205-213

[4] FFDNet: Toward a Fast and Flexible Solution for CNN based Image Denoising.[J] . Zhang Kai, Zuo Wangmeng,Zhang Lei. IEEE transactions on image processing: a publication of the IEEE Signal Processing Society. 2018

[5] Guo Zhonghua, Li Shuqing, Wang Lei, et al. Research on improved wavelet denoising algorithm based on adaptive threshold [J]. Journal of Chongqing University of posts and Telecommunications (Natural Science Edition), 2015,27 (6): 740-744750.

[6] Jiang Huawei, Yang Zhen, Zhang Xin,Dong Journal of Jilin University (Engineering Edition): 1-14 [2021-05-09].

[7] Liu Lijun, Chen Zhen Evaluation method of atomized image restoration effect based on relative contrast and edge similarity [J]. Journal of Beihua University (Natural Science Edition). 2016pr 17 (06)

[8] A new construction land extraction method based on improved U-net network [J]. Liang Zhe, Ning Xiaogang, Zhang Hanchao, Wang Hao. Remote sensing information. 2020 (03)

[9] Xie Fengyun, Zhou Jianmin, Jiang Weiwen, et al. Research on Apple grading method based on Hidden Markov Model [J]. Food and Machinery, 201632 (7): 2931111

[10] Huang Chen, Fei Jiyou. Apple online grading method based on image feature fusion [J]. Journal of Agricultural Engineering, 2017,33 (1): 285-291.

[11] Zeng Jun. Research on Image Edge Detection Technology and its Application [D]. Wuhan: Huazhong University of Science and Technology, 2011.

[12] Xing Xiaomin, Liu Wei. De-fog of a single image in a foggy traffic scene [D]. Chinese Journal of Image and Graphics, 2016, 21 (11): 1440-1447.

[13] Loss Functions for Image Restoration With Neural Networks[J] . Zhao Hang, Gallo Orazio, Frosio Iuri, Kautz Jan. IEEE Transactions on Computational Imaging. 2017 (1)

[14] KANG X, STAMN M C, PENG A, et al. Robust medianfiltering forensics based on the autoregressive model of medianfiltered residual [C]// Signal & Information Processing Association Summit & Conference. IEEE, 2012.

[15] DehazeNet: An End-to-End System for Single Image Haze Removal. [J] . Bolun Cai, Xiangmin Xu, Kui Jia, Chunmei Qing, Dacheng Tao. IEEE transactions on image processing: a publication of the IEEE Signal Processing Society. 2016 (11)

[16] Image Dehazing Using Residual-Based Deep CNN[J]. Li Jinjiang, Li Guihui, Fan Hui. IEEE Access. 2018

[17] Xu Tao, Wu Qian, Niu Haiqing, et al. An improved infrared image edge extraction algorithm for porcelain sleeve cable terminal [J]. Electric porcelain Lightning arrester, 2016 (6): 26-31

[18] Liu Jieping, Huang Bingkun, Wei Gang. a fast single image defog algorithm [J]. Acta Electronica Sinica, 2017. 45 (8): 1896-1901.

[19] Zhang Xiaolin, Jing Yuefeng, Liu Jun. Edge detection method of Sobel operator in high energy flash illumination [J]. Journal of remote Sensing. 2006 10 (5): 357

Caishu Li is currently studying for a master's degree at Shenyang University of Construction Control Science and Engineering, China. In 2019, he graduated from Shenyang building automation major with a bachelor's degree. The main research direction is computer vision and image processing, and his main research is image recognition and enhancement processing of power equipment.

Liu Jian is a professor at Shenyang Institute of Building Information and Control Engineering. After graduating from university in 1983, he was engaged in the research and development of control engineering application projects in Shenyang Research Institute and completed a number of large-scale engineering research projects. He graduated from Northeast Automatic Control University in 1996 and had academic exchanges at Tampere University of Technology in Finland. Since 1988, he has been engaged in the teaching and research of control theory and control engineering at Shenyang Jianzhu University.